Journal of Applied Research in Water and Wastewater
E-ISSN: 2476-6283
Journal homepage: https://arww.razi.ac.ir

Synthesis and optimization of biochar prepared from cow dung for methylene blue removal

Zohreh Jahannia, Hassan Rezaei*, Hajar Abyar, Somayeh Namroodi

Department of Environmental Sciences, Faculty of Fisheries and Environmental Sciences, Gorgan University of Agricultural Sciences and Natural Resources, Gorgan, Iran.

GRAPHICAL ABSTRACT

ARTICLE INFO

Article type:
Research Article

Article history:
Received xx Month xxx
Received in revised form xx Month xxx
Accepted xx Month xxx
Available online x Month xx

Keywords:
Methylene blue
Cow dung
Biochar
Aqueous solutions
Adsorption kinetics

ABSTRACT

Cost-effective dye wastewater treatment approaches are critically required for the long-term sustainability of textile industries. To fill the gaps, multiple high-potential adsorbents derived from biomass have been proposed. For this purpose, this study was conducted to present an applicable and cost-effective biochar synthesized from cow dung to remove methylene blue from the aqueous solutions. The potential of cow dung-based biochar was optimized under various pH, biochar dose, methylene blue concentration, contact time, and temperature. The maximum removal was 96% achieved at optimum conditions, 20 mg/l methylene blue concentration, 0.2 g biochar dose, pH of 6, and 90 min contact time at ambient temperature. The methylene blue adsorption process followed the Freundlich isotherm (R^2=0.9827) and pseudo-second-order (R^2=0.999) kinetic models, implying multilayered adsorption on the heterogenous surface and chemisorption mechanism, respectively. Furthermore, the adsorption process was spontaneous and exothermic due to negative Gibbs free energy (ΔG^0) and enthalpy (ΔH^0) with the reduction at randomness of methylene blue molecules and adsorbent interaction based on negative entropy (ΔS^0). Regarding the high efficiency of cow dung-based biochar to adsorb methylene blue, it is recommended that further investigations consider the biochar activation and functionalization intending to upgrade its adsorption capacity.

1. Introduction

The increasing release of dyes into the environment due to the expansion of industrial activities is one of the critical challenges at the global level (Li *et al*., 2017). Regarding the detrimental effects of dyes on human health and aquatic life, the removal of dyes from wastewater before discharge into the natural habitat is indispensable (Ahmad *et al.*, 2020a). Methylene blue, methyl orange, rhodamine B, crystal violet, Congo red, and diffuse violet produced from azo, thioquinone, and xanthan are the most significant and toxic dyes in industrial and non-industrial effluents. They are non-biodegradable and mutagenic, hindering sunlight penetration into the water and damaging aquatic organisms (Valderrama *et al.*, 2010; Bayahia, 2022). Successive exposure to methylene blue as a cationic molecule leads to sensory system problems, skin sensitivities, and cardiovascular and human respiratory damage (Udayakumar *et al.,* 2021). Therefore, dye

*Corresponding author Email: hassanrezaei@gau.ac.ir

Cite this article: Z. Jahannia, H. Rezaei, H. Abyar, S. Namroodi, Synthesis and optimization of biochar prepared from cow dung for methylene blue removal, *Journal of Applied Research in Water and Wastewater*, x (x), 202x, xx-xx. doi: https://doi.org/10.22126/arww.2024.10163.1320

concentrations in the effluent should be managed efficiently to avoid environmental crises (Putranto *et al.*, 2022).

Advanced oxidation processes, adsorption, membrane filtration, coagulation, and ion exchange have been proposed for dye removal. However, adsorption methods are at the heart of consideration due to their versatility, adjustability, and wide variety of available adsorbents (Baloo *et al*., 2021). The efficiency of the adsorption process strongly depends on the adsorbent characteristics, wastewater composition, and the analyte type (Misran *et al.*, 2022). Carbonized char as an applicable adsorbent can adsorb dyes through chemical or physical bonding on the surface. The adsorption quality is related to pore volume, surface area, pore diameter, and size distribution. A slight change in these characteristics considerably increases the char adsorption capacity (Ofgea, Tura, and Fanta, 2022).

The char synthesis from natural and low-cost agricultural waste such as orange peel, banana peel, peanut peel, lemon peel, coconut shell, and bamboo branches has been conducted for dye removal *(Yusop et al*., 2021). Biochar is a high-potential material produced from different available biomass (Yusop, Aziz, and Ahmad, 2022). The biochar porosity captures the dye molecules and can be regenerated accordingly (de Souza *et al.*, 2022). The morphology and size distribution of the pores on the surface affects the adsorption rate (Alshekhli *et al.,* 2020).

Cow dung is a cost-effective and readily available biological resource. Traditional applications of cow dung such as burning as fuel, mosquito repellants, and cleaning agents are already presented (Saraswat, Demir, and Gosu, 2020). The recent development of cow dung is attributed to biofuel production or environmental pollution management. Cow dung is also a practical alternative for the adsorption process because of its affordability and the possibility of recovery, mass production, and availability (Iwuozor *et al.*, 2022). On the other hand, cow dung is used to remove pollution due to its high carbon content, suitable porosity, and high efficiency (Jain *et al*., 2022). Notably, the dung of horses, cows, sheep, and chickens contains organic substances, enriching farm soils (Pandey *et al.*, 2021). It is animal manure, and its properties lead to increased permeability and water retention, improved aeration, and stimulating the biological activity of the soil (Iwuozor *et al.*, 2022).

According to the limited investigations in terms of cow dung adsorption potential, the present study was conducted to comprehensively evaluate the cow dung's capability and capacity to remove methylene blue from aqueous solutions. The impacts of temperature, contact time, methylene blue concentration, biochar dose, and pH on the biochar performance were also considered to attain the optimum conditions. Isotherm, kinetic, and thermodynamic modeling were also applied to analyze the adsorption mechanism. The results of this study can provide an innovative pathway toward green sustainable development.

2. Materials and methods

2.1. Sample collection

Cow dung was collected from industrial cattle farms and dried in an oven for 24 hours at a temperature of 110 °C and then powdered (Pandey *et al.*, 2021). The elemental analysis showed the amount of carbon, nitrogen, sulfur, and hydrogen as 31.19%, 2.41%, 0.711%, and 3.66%, respectively.

2.2. Biochar preparation

20 g of as-prepared powder was pyrolyzed in the furnace (TF5/25-1250) for one hour at a temperature of 500 °C and a heating rate of 10 ml/min under the nitrogen gas flow with a pressure of 100 ml/min (Saraswat, Demir, and Gosu, 2020).

2.3. Biochar characterization

The elemental analysis was carried out using an elemental analyzer (Flash EA 1112, USA). Field scanning electron microscopy analysis (SEM, Model: FEIESEM QUANTA200) was applied to determine the size and morphology of the cow dung-based biochar. Fourier-transform infrared spectroscopy (FTIR; Thermo Nicolet Avatar 370 FTIR, USA) was also performed to assess the surface functional groups of biochar.

2.4. Optimization of methylene blue removal

The operational parameters including temperature, contact time, methylene blue concentration, biochar dose, and pH were selected to optimize methylene blue removal using the one-at-a-time method (Ahmad *et al.*, 2020a; Bayahia, 2022). The biochar potential for methylene blue removal was evaluated at pH values of 4, 6, 8, 10, and 12 with a biochar dose of 0.2 g, contact time of 1 hour, and methylene blue concentration of 10 mg/l at a temperature of 25 °C (Ahmad *et al.*, 2020a). Then, the experiment was performed at a biochar dose of 0.2, 0.3, 0.5, 0.7, and 1 g, while pH, methylene blue concentration, temperature, and contact time were 6, 10 mg/L, 25 °C, and 1 h, respectively. Methylene blue concentration was optimized at 5, 10, 20, 50, and 100 mg/l at a contact time of 1 h, temperature of 25 °C, biochar dose of 0.2 g, and pH = 6. The experiment was repeated at the contact time of 15, 30, 60, 90, and 120 min with 0.2 g biochar dose, at a temperature of 25 °C, optimum methylene blue concentration of 20 mg/l, and pH= 6. Finally, the biochar capability in methylene blue removal was assessed at the temperature of 10, 15, 20, 30, and 40 °C under pH=6, 0.2 g biochar dose, 90 min optimum contact time, and 20 mg/l methylene blue concentration. The experiments were carried out in three replicates. The adsorption capacity and removal percentage were calculated using the following formulas:

$$\mathrm{Qe} = (\mathrm{C_i} - \mathrm{C_f}) \times \frac{\mathrm{V}}{\mathrm{M}} \quad (1)$$

$$\mathrm{A\%} = \frac{(\mathrm{C_i} - \mathrm{C_f})}{\mathrm{C_i}} * 100 \quad (2)$$

where, Q_e is adsorption capacity. C_i and C_f denote primary and final methylene blue concentrations. V and M are the solution volume and biochar dose, respectively. A also indicates the removal percentage.

2.5. Isotherm modeling

Adsorption characteristics are expressed by adsorption equilibrium isotherms (Vyawahare *et al.*, 2022). Adsorption isotherms are invaluable parameters indicating adsorbate mobility from the bulk solution to a solid phase at a constant pH and temperature (Nowrouzi, Younesi, and Bahramifar, 2018; Peer, Bahramifar, and Younesi, 2018). Moreover, when adsorbate concentration in aqueous media is balanced with the adsorbed ones on the adsorbent, the equilibrium condition is established (Ayawei, Ebelegi, and Wankasi, 2017). Langmuir and Freundlich isotherm models were used in this study to specify the adsorption of methylene blue molecules on cow dung-based biochar. Langmuir presents the adsorption isotherm based on the equality of adsorption and desorption rates as follows (Majd *et al.*, 2022):

$$\frac{C_e}{q_e} = \frac{1}{q_m} C_e + \frac{1}{q_m b} \quad (3)$$

where q_e and q_m denote the equilibrium and maximum adsorption capacity (mg/g), respectively. b depicts the Langmuir constant and C_e is the equilibrium concentration of adsorbate (mg/L). The basic characteristic of the Langmuir isotherm model is the dimensionless constant called R_L (Langmuir separation factor), which is defined by the following equation:

$$\mathrm{R_L} = \frac{1}{(1+\mathrm{bC_0})} \quad (4)$$

where, b and C_0 are the Langmuir constant and the initial adsorbate concentration (mg/L), respectively. R_L indicates the type of isotherm as irreversible (R_L=0), favorable (0<RL<1), linear (R_L=1), and unfavorable (R_L>1) (Latour, 2015). Freundlich isotherm is based on multi-layered and heterogeneous adsorption of the substance on the absorbent and is described as follows (Rajahmundry *et al.*, 2021):

$$\mathrm{Ln_{qe}} = \mathrm{Ln_{KF}} + \frac{1}{\mathrm{n}} \mathrm{Ln_{Ce}} \quad (5)$$

where, k_F and 1/n denote the Freundlich constant and exponent, respectively. The index 1/n shows the Freundlich intensity parameter and the experimental conditions are favorable when 1/n<1.

2.6. Adsorption kinetics

To determine the optimal contact time and predict the speed of the adsorption process, adsorption kinetic models were investigated (Gorissen *et a*l., 2020). Kinetics equations manifest the adsorption mechanism and contributed processes such as surface, intermolecular, and chemical adsorption as well as diffusion (Li *et al*., 2022). The shorter the contact time in the adsorption process, the higher the reaction speed, which is cost-effective from an economic point of view (Liu et al., 2020). The pseudo-first-order kinetic model elucidates that the changes in the adsorption rate with time are proportional to the unoccupied sites on the surface of the absorbent (Song et al., 2020).

$$\ln(q_e - q_t) = lnq_e - k_1 t \quad (6)$$

where, k_1 shows the pseudo-first-order rate constant (1/min) and q_t depicts the adsorption capacity at time t. The pseudo-second-order

kinetic model assumes that chemical adsorption controls the adsorption phenomenon and the rate of adsorption site occupation is related to the square of the unoccupied sites (Hu *et al*., 2020).

$$\frac{t}{q_t} = \frac{1}{K_2 qe_2^2} + \frac{1}{qe_2} t \quad (7)$$

where, k_2 is the pseudo-second-order constant rate and t is the time (min).

2.7. Adsorption thermodynamics

Thermodynamic parameters including Gibbs free energy changes (ΔG°), standard enthalpy (ΔH°), and standard entropy (ΔS°) can be obtained using the following equations (Shukre *et al*., 2022):

$$\Delta G^0 = -RTLnK_d \quad (8)$$

$$\Delta G^0 = \Delta H^0 - T\Delta S^0 \quad (9)$$

$$LnK_D = -\frac{\Delta H^0}{RT} + \frac{\Delta S^0}{R} \quad (10)$$

where, R is the global constant of gases with a value of 8.314 J/K.mol. T is the absolute temperature (K), and K_d is the equilibrium constant (Brandani, 2022).

3. Results and discussion

3.1. Characterization

The morphology of the biochar prepared from cow dung was investigated using SEM analysis. Fig. 1 shows that the surface of synthesized biochar is thick and porous with small holes. The FTIR spectrum of cow dung-based biochar is exhibited in Fig. 2. As can be seen, broad peaks at 3429.32 cm^{-1} and 3126.08 cm^{-1} indicate the O-H stretching vibration (Xiu et al., 2020). The weak absorption peak in 3310 cm^{-1} is the N-H bond of the stretching (Tang et al., 2021). The peak at 1638.82 cm^{-1} is related to the C=O bond (Patty, Loupatty, and Sopalauw, 2017). The sharp peaks at 1453.27 cm^{-1} and 1400.19 cm^{-1} correspond to the asymmetric C–H bending vibrations and CH_3 bending, respectively (Rani et al., 2017; Tang et al., 2022). The stretching vibration of C-O is at 1071.62 cm^{-1} (Khoon Poh et al., 2014)

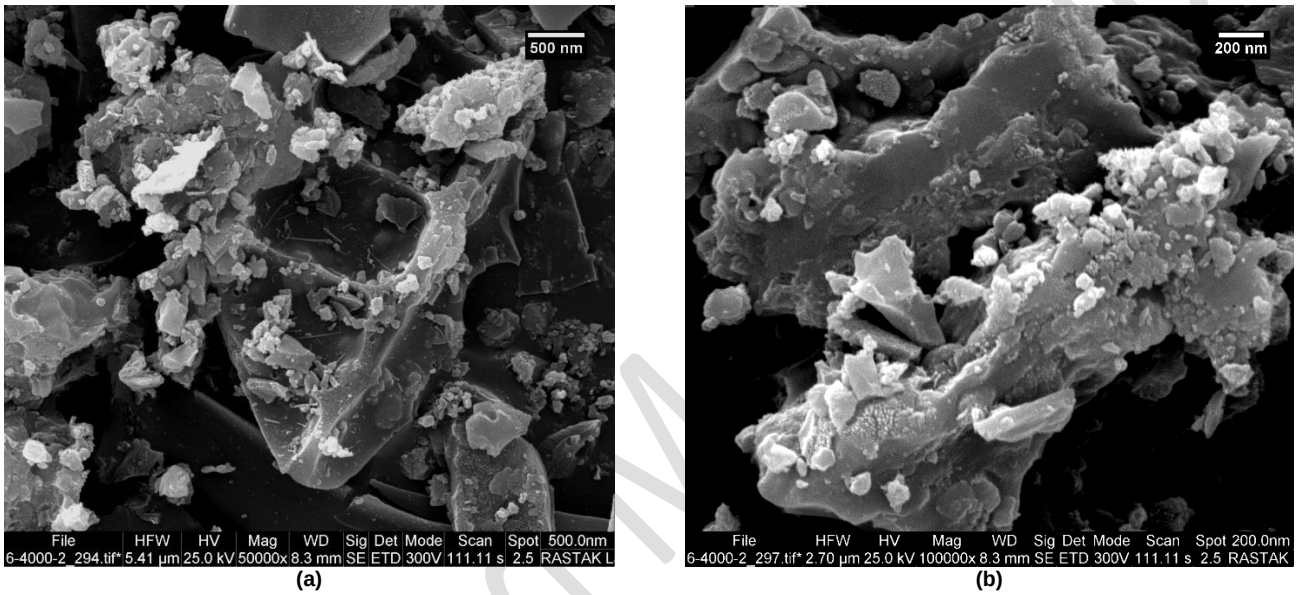

(a) **(b)**

Fig. 1. SEM image of cow dung-based biochar, (a) 50 and (b) 100 kx magnification.

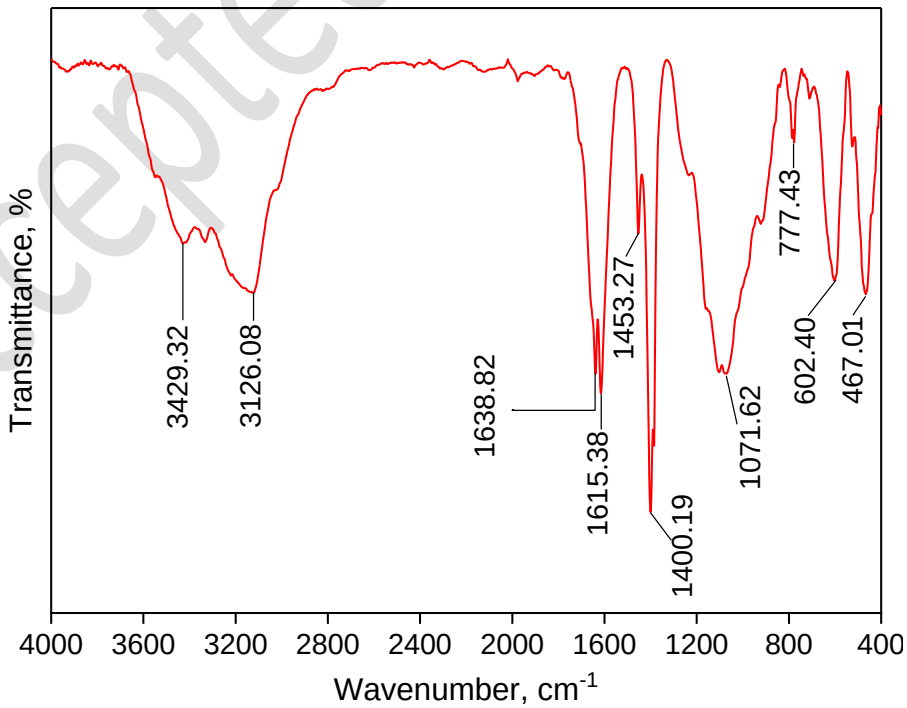

Fig. 2. FTIR spectrum of cow dung-based biochar.

3.2. Effect of pH

The effect of pH in the range of 4-12 on methylene blue adsorption is shown in Fig. 3a, while other parameters were fixed at 0.2 g adsorbent dose, 1 h contact time, 10 mg/l methylene blue concentration, and room

temperature. According to the obtained results, the trend of methylene blue removal at various pH depicted more fluctuations. However, the maximum methylene blue removal was detected at pH=4 equivalent to 93.08% with an adsorption capacity of 3.07 mg/g. It should be mentioned that solution pH can directly affect the biochar surface charge and the degree of ionization of pollutants. At acidic conditions, H^+ ions compete with cationic methylene blue molecules to be adsorbed by biochar. Then, the H^+ ions induce the biochar surface to be positively charged, creating a repulsion force between the biochar surface and methylene blue ions (Habeeb *et al*., 2023). However, the adsorption capacity of methylene blue was enhanced by the pH increase due to the weak impact of H^+ on the charge of the biochar surface (Ofgea, Tura, and Fanta, 2022; Yusop, Aziz, and Ahmad, 2022). A similar finding was obtained by Chu et al. (2019) who reported the maximum removal efficiency of rhodamine B (97.7%) at pH 4 using sodium dodecyl sulfate-modified nano-alumina. Another study revealed the significant decolorization of methylene blue at about 77% at pH 3 after 30 min (Sun *et al*., 2015).

3.3. Effect of biochar dose

The adsorption process of methylene blue at a biochar dose of 0.2 to 1 g is demonstrated in Fig. 3b. The other parameters were fixed at a pH of 6, contact time of 1 h, methylene blue concentration of 10 mg/L, and room temperature. The highest adsorption capacity (4.10 mg/g) was obtained at 0.2 g biochar dose with a removal efficiency of 82.08%. As can be seen, the removal efficiency of cow dung-based biochar increased from 82.08% to 96.95% while the biochar dose was enhanced. This can be attributed to the more available adsorption sites for methylene blue molecules. Ahmad *et al*. (2020b) also reported the adsorption efficiency of methylene blue as 91.3% at 0.5 gm/100 mL of cow dung biochar dose. Another study indicated the enhancement of methylene blue removal rate from 47.76% to 98.95% while the dose of cattle manure-derived low-temperature biochar was increased from 0.01 g to 0.5 g, which was relevant to the availability of more adsorption sites and increased adsorbent surface area (Zhu *et al*., 2018). Moreover, Habeeb, Zinatizadeh and Zangeneh (2023) declared that the increase in the B-ZnO/TiO_2 photocatalyst loading from 0.5 g/l to 1.5 g/l led to the enhancement of dye removal from 40% to 70%. However, a reduction of adsorption capacity was observed from 4.10 mg/g to 0.97 mg/g with the increase of the adsorbent dose. Rapid superficial sorption onto the cow dung-based biochar occurred at a higher adsorbent dose, whereas lower methylene blue molecules were adsorbed per available adsorption sites, leading to lower adsorption capacity (Einollahipeer, and Okati, 2022; Subramaniam, and Ponnusamy, 2015). Another reason for the reduction of adsorption capacity at a fixed methylene blue concentration could be related to the aggregation of adsorbent particles that decreased the total surface area and increased the diffusional path (Shirmardi *et al*., 2016; Zhu *et al*., 2018).

3.4. The effect of the initial methylene blue concentration

The impact of methylene blue concentration was assessed in the range of 5-100 mg/l at fixed pH=6, contact time of 1 hour, biochar dose of 0.2 g, and room temperature. As can be seen in Fig. 4a, while the methylene blue concentration was enhanced to 100 mg/l, the adsorption efficiency dropped from 93.27% to 69.07%. The rapid removal of methylene blue at the beginning was probably associated with the great number of available vacant sites, which gradually decreased to attain equilibrium conditions (Rezaei, Rostami, and Abyar, 2024). The maximum adsorption capacity was achieved at 100 mg/l methylene blue equivalent to 9.87 mg/g. Generally, the transfer rate of methylene blue molecules on the adsorbent accelerates by increasing of dye concentration, which results in a high adsorption capacity (de Souza et al., 2022). According to the literature (Alshekhli *et al.*, 2020), the initial concentration of methylene blue provides a strong driving force to overcome the mass transfer resistance between the aqueous and solid phases, leading to high adsorption capacity.

3.5. Effect of contact time

The effect of contact time on the adsorption process in a range of 15 to 120 min is manifested in Fig. 4b at pH=6, temperature of 25 °C, biochar dose of 0.2 g, and methylene blue concentration of 20 mg/L. The maximum removal was achieved at 120 min equal to 92.51% with an adsorption capacity of 2.64 mg/g. As can be seen, the methylene blue adsorption showed a slight reduction at the initial 30 min and then increased with contact time enhancement. This can be explained that at the beginning of the adsorption process, a large number of empty sites are available on the biochar surface and the adsorption of methylene blue dye shows an increasing trend until stabilized (Ahmad *et al*., 2020b; Habeeb, Zinatizadeh, and Zangeneh, 2023). Abd-Elhamid *et al*. (2020) also demonstrated the increase of methylene blue and crystal violet removal with time with maximum adsorption efficiency of 99.91 and 44.64 mg/g, respectively. The same trend was found by Subramaniam and Ponnusamy (2015) for methylene blue removal, which rapidly increased with time more than 60 min. They also referred to the aggregation of dye molecules at the high contact time, hindering the deeper diffusion into the adsorbent structure, and the pores get filled up (Subramaniam, and Ponnusamy, 2015).

3.6. Effect of temperature

Fig. 4c shows the effect of temperature on the adsorption process in the range of 10-40 °C at pH=6, the contact time of 90 min, biochar dose of 0.2 g, and methylene blue concentration of 20 mg/L. The maximum methylene blue removal (98.78%) was obtained at a temperature of 10 °C with an adsorption capacity of 2.69 mg/g. A decreasing trend in methylene blue adsorption was observed with a temperature increase from 10 °C to 40 °C. However, the effect of temperature on the adsorption capacity was smaller and showed only a 3.7% reduction in the temperature range from 10 to 40 °C, demonstrating the capability of the cow dung-based biochar for wastewater treatment at ambient temperature (Zhu *et al*., 2018). Moreover, high temperatures enhance the mobility of methylene blue molecules, further decrease their penetration to the adsorbent pores, and reduce the adsorption potential (Ramutshatsha-Makhwedzha et al., 2022). The results were consistent with the literature (Yusop *et al*., 2021; Putranto *et al*., 2022). Notably, the cow dung-based biochar could maintain 70% of its capacity after 20 cycles.

3.7. Isotherm modeling

The correlation coefficients and adsorption parameters of Langmuir and Freundlich isotherm models are shown in Fig. 5 and Table 1. Isotherm of methylene blue adsorption on cow dung-based biochar fitted well with the Freundlich model (R^2=0.9827) which elucidated a heterogeneous surface of the biochar with multilayer adsorption accompanied by the exponential distribution of adsorbent active sites (Rastgar *et al*., 2023; Saleh, 2022). K_F and 1/n values were 1.39 and 0.572, respectively, which revealed a favorable non-linear interaction of dye adsorption (Nowrouzi *et al*., 2017; Rastgar *et al*., 2022). On the other hand, the Langmuir isotherm showed a q_m value of 12.25 mg/g with an R^2 of 0.9186. Moreover, the R_L constant value of 0.299 confirmed the favorable adsorption of methylene blue. Regarding the Freundlich graph (Fig. 5b), the isotherm of methylene blue adsorption on cow dung-based biochar was C-type, implying that the ratio between the adsorbed dye molecules onto the adsorbent surface area and dye molecules concentration in solution was proportionally at any concentration (Baloo *et al*., 2021).

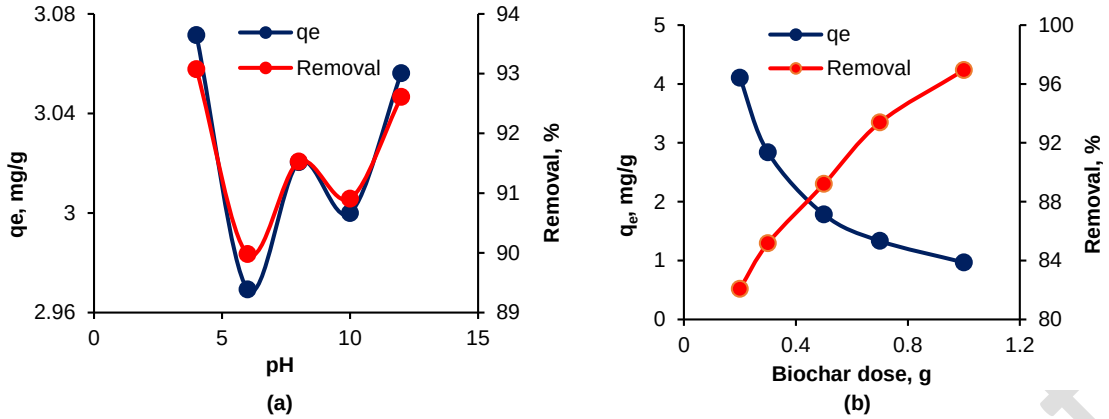

Fig. 3. Removal of methylene blue at different pH (a) and adsorbent dose (b).

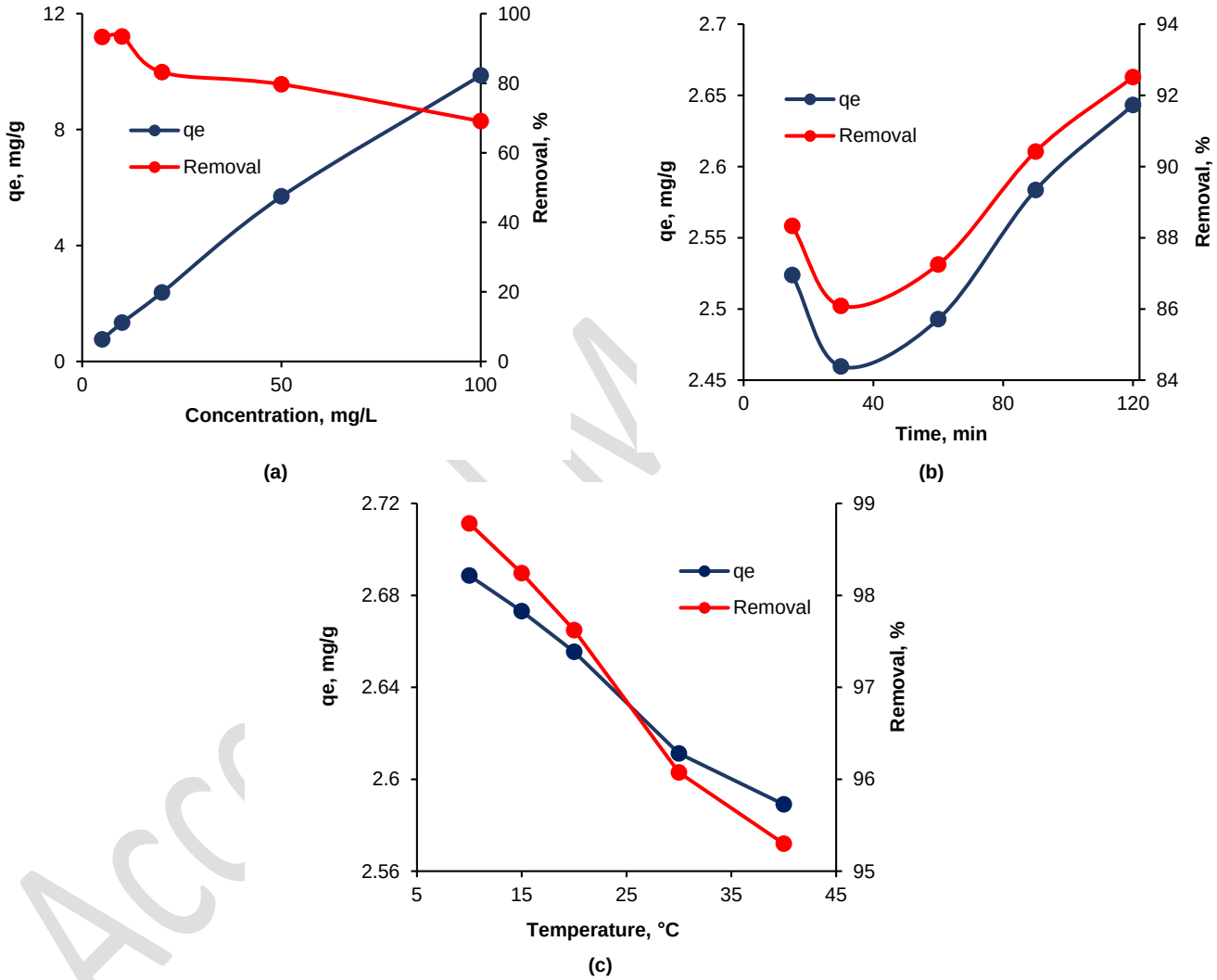

Fig. 4. The effect of methylene blue concentration (a), contact time (b), and temperature (c) on the methylene blue removal.

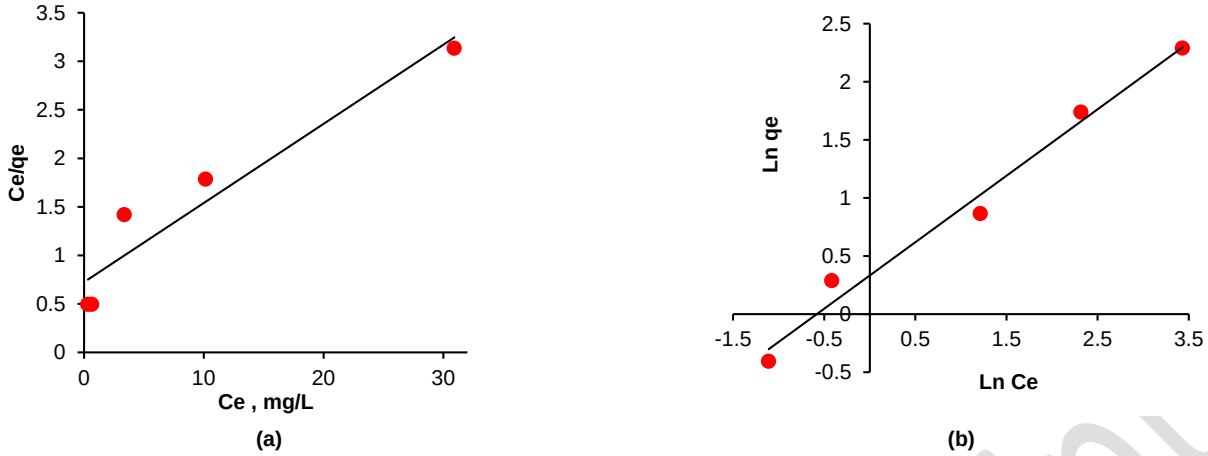

Fig. 5. (a) Langmuir and (b) Freundlich isotherm models for methylene blue adsorption.

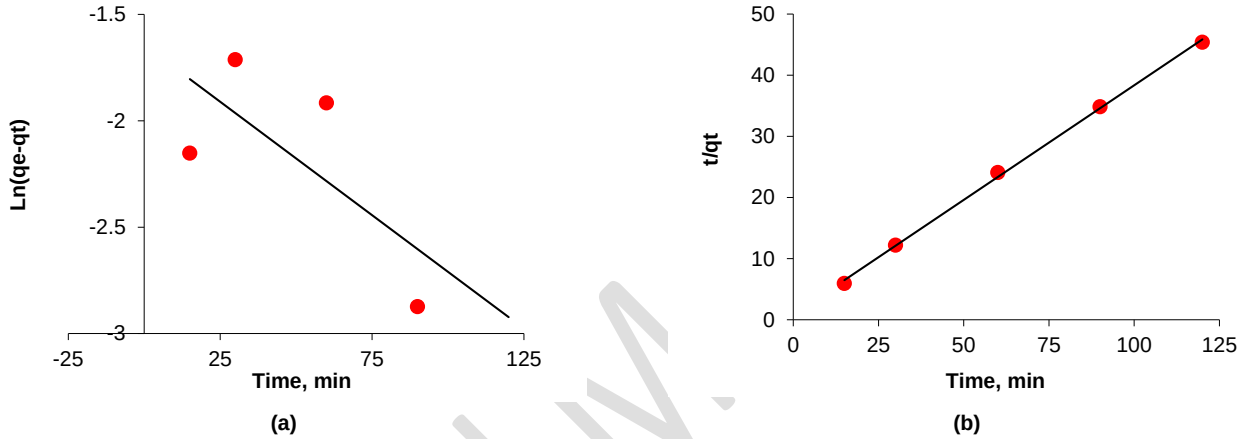

Fig. 6. Pseudo-first (a) and second-order (b) kinetic models.

Table 1. Comparison of isotherm and kinetics of the adsorption process using cow dung-based adsorbents.

Isotherm	**Langmuir**				**Freundlich**			
Pollutant	**q_{max}, mg/g**	**B, L/mg**	**R^2**	**R_L**	**K_F, $(mg/g)(L/mg)^{1/n}$**	**n**	**R^2**	**Reference**
Methylene blue	12.25	0.117	0.9186	0.299	1.39	1.75	0.9827	This study
Methylene blue	17.506	0.583	0.996	0.017	-	<1	0.927	(Ahmad *et al*., 2020b)
Methylene blue	192.31	0.1763	0.9999	0.102	39.91	2.66	0.8887	(Zhu *et al*., 2018)
Glyphosate	-	-	-	-	1.168	3.293	0.985	(Garba *et al*., 2019)
AMPA*	-	-	-	-	2.915	2.119	0.865	(Garba *et al*., 2019)
Cadmium	5.12	1.67	0.93	0.009	2.54	6.25	0.91	(Van Phuong, and Hoang, 2021)
Fluoride	83.83	0.084	0.781	0.39	8.18	0.89	0.947	(Rajkumar *et al*., 2019)
Kinetic	**Pseudo-first order**				**Pseudo-second order**			
Pollutant	**q_e, mg/g**	**k_1, min^{-1}**	**R^2**		**q_e, mg/g**	**k_2, g/mg min**	**R^2**	**Reference**
Methylene blue	2.64	0.01	0.4895		2.66	0.164	0.999	This study
Methylene blue	13.876	0.018	0.925		19.157	0.023	0.994	(Ahmad et al., 2020b)
Methylene blue	39.01	0.017	0.9944		39.15	0.026	1	(Zhu et al., 2018)
Methylene blue	-	-	-		35.59	0.0042	0.922	(Tsai, Hsu, and Lin, 2019)
Fluoride	16.37	0.0394	0.967		4.69	0.0743	0.993	(Rajkumar et al., 2019)
Cadmium	1.58	0.015	0.91		4.73	0.055	0.8	(Van Phuong, and Hoang, 2021)

Aminomethylphosphonic acid

Table 2. Thermodynamic parameters of methylene blue adsorption.

T, K	ΔG^0, $kJ.mol^{-1}$	ΔH^0, $kJ.mol^{-1}$	ΔS^0, $J.mol^{-1}.K^{-1}$
283	-1911.31	-12944.9	-39.079
288	-1715.89		
293	-1493.08		
303	-1001.03		
303	-795.041		

3.8. Adsorption kinetics

The rate constants of the adsorption process were ascertained using pseudo-first and second-order kinetic models to evaluate the adsorption mechanisms. The acquired plots and coefficients are indicated in Fig. 6 and Table 1. The pseudo-second-order kinetic model with an R^2 of 0.999 was well-fitted with the empirical data which proved that the chemisorption reaction controlled the methylene blue adsorption (Tran, 2022). The value of q_e was 2.66 mg/g with K_2 of 0.164. Adsorption of phenol (Jain *et al.*, 2022), organic pollutants (Chen *et al*., 2022), and methylene blue (Kandasamy *et al*., 2023) by cow dung-

based adsorbents also followed the pseudo-second-order kinetic model.

3.9. Adsorption thermodynamics

In order to study the temperature influence on the adsorption process, thermodynamic parameters were calculated which are listed in Table 2. A negative ΔG^o value was indicative of the spontaneity of the adsorption process. ΔH^o presented the negative value which referred to the exothermic adsorption process (Jain *et al*., 2022). The negative value of ΔS^o also indicated a reduction in the randomness at the adsorbent/solution interface within the adsorption process (Sahmoune, 2019).

4. Conclusions

This study evaluated the potential of synthesized biochar derived from cow dung for methylene blue removal. The optimum pH, biochar dose, initial methylene blue concentration, contact time, and temperature were 6, 0.2 g, 20 mg/L, 90 min, and ambient temperature. The maximum adsorption capacity was accounted as 12.25 mg/g. The adsorption process was heterogeneous, chemical, and spontaneous based on isotherm, kinetic, and thermodynamic studies. The negative ΔH^o values elucidated the exothermic adsorption process. The superiority of this study was to highlight the intrinsic potential of cost-effective and available cow dung waste as a precursor for methylene blue removal. However, the feasibility of cow dung-based biochar application in an industrial aspect should be explored from environmental and economic points of view.

Author Contributions

Zohreh Jahannia: Conceptualization, investigation, methodology, and writing-original draft.
Hassan Rezaei: Supervision, validation, review, and editing.
Hajar Abyar: Investigation, methodology, analysis, review, and editing.
Somayeh Namroodi: review and editing.

Conflict of Interest

The authors declare no competing interests and non-financial competing interests.

Acknowledgments

The authors would like to thank Gorgan University of Agricultural Sciences and Natural Resources, Iran, for their support.

Data Availability Statement

The datasets used and/or analyzed during the current study are available from the corresponding author on reasonable request.

References

Abd-Elhamid, A. *et al.* (2020) 'Enhanced removal of cationic dye by eco-friendly activated biochar derived from rice straw', *Applied Water Science,* 10**,** pp. 1-11. doi: https://doi.org/10.1007/s13201-019-1128-0

Ahmad, A. *et al.* (2020a) 'A novel study on synthesis of egg shell based activated carbon for degradation of methylene blue via photocatalysis', *Arabian Journal of Chemistry,* 13**,** pp**.** 8717-8722. doi: https://doi.org/10.1016/j.arabjc.2020.10.002

Ahmad, A. *et al.* (2020b) 'Removal of methylene blue dye using rice husk, cow dung and sludge biochar: Characterization, application, and kinetic studies', *Bioresource technology,* 306**,** pp. 123202. doi: doi: https://doi.org/10.1016/j.biortech.2020.123202

Alshekhli, A. F. *et al.* (2020) 'Development of adsorbent from phytoremediation plant waste for methylene blue removal', *Journal of Ecological Engineering,* 21**,** pp. 207-215. doi: https://doi.org/10.12911/22998993/126873

Ayawei, N.,Ebelegi, A. N., and Wankasi, D. (2017) 'Modelling and interpretation of adsorption isotherms', *Journal of chemistry,* 2017**,** pp. 1-11. doi: https://doi.org/10.1155/2017/3039817

Baloo, L. *et al.* (2021) 'Adsorptive removal of methylene blue and acid orange 10 dyes from aqueous solutions using oil palm wastes-derived activated carbons', *Alexandria Engineering Journal,* 60**,** pp. 5611-5629. doi: https://doi.org/10.1016/j.aej.2021.04.044

Bayahia, H. (2022) 'Green synthesis of activated carbon doped tungsten trioxide photocatalysts using leaf of basil (Ocimum basilicum) for photocatalytic degradation of methylene blue under sunlight', *Journal of Saudi Chemical Society,* 26**,** pp. 101432. doi: https://doi.org/10.1016/j.jscs.2022.101432

Brandani, S. (2022) 'The rigid adsorbent lattice fluid model: thermodynamic consistency and relationship to the real adsorbed solution theory', *Membranes,* 12**,** pp. 1009. doi: https://doi.org/10.3390/membranes12101009

Chen, X. *et al.* (2022) 'Cow dung-based biochar materials prepared via mixed base and its application in the removal of organic pollutants', *International Journal of Molecular Sciences,* 23**,** pp. 10094. doi: https://doi.org/10.3390/ijms231710094

Chu, T. P. M. *et al.* (2019) 'Synthesis, characterization, and modification of alumina nanoparticles for cationic dye removal', *Materials,* 12**,** pp**.** 450. doi: https://doi.org/10.3390/ma12030450

de Souza, C. C. *et al.* (2022) 'Activated carbon of *Coriandrum sativum* for adsorption of methylene blue: Equilibrium and kinetic modeling', *Cleaner Materials,* 3**,** pp. 100052. doi: https://doi.org/10.1016/j.clema.2022.100052

Einollahipeer, F., and Okati, N. (2022) 'High efficient Hg (II) and TNP removal by NH_2 grafted magnetic graphene oxide synthesized from Typha latifolia', *Environmental Technology,* 43**,** pp. 3956-3972. doi: https://doi.org/10.1080/09593330.2021.1937708

Garba, J. *et al.* (2019) 'Evaluation of adsorptive characteristics of cow dung and rice husk ash for removal of aqueous glyphosate and aminomethylphoshonic acid', *Scientific reports,* 9**,** pp. 17689. doi: https://doi.org/10.1038/s41598-019-54079-0

Gorissen, S. H. *et al.* (2020) 'Protein type, protein dose, and age modulate dietary protein digestion and phenylalanine absorption kinetics and plasma phenylalanine availability in humans', *The Journal of nutrition,* 150, pp. 2041-2050. doi: https://doi.org/10.1093/jn/nxaa024

Habeeb, S. *et al.* (2023) 'Visible light activated fe-n-sio_2/tio_2 photocatalyst: providing an opportunity for enhanced photocatalytic degradation of antibiotic oxytetracycline in aqueous solution', *International Journal of Engineering,* 36**,** pp**.** 615-629. doi: https://doi.org/10.5829/ije.2023.36.04a.02

Habeeb, S.A., Zinatizadeh, A.A., Zangeneh, H. (2023) 'Photocatalytic decolorization of direct red16 from an aqueous solution using B-ZnO/TiO_2 nano photocatalyst: synthesis, characterization, process modeling, and optimization', *Water,* 15**,** pp**.** 1203. doi: https://doi.org/10.3390/w15061203

Hu, H. *et al.* (2020) 'Comparative absorption kinetics of seven active ingredients of Eucommia ulmoides extracts by intestinal in situ circulatory perfusion in normal and spontaneous hypertensive rats', *Biomedical Chromatography,* 34**,** pp**.** e4714. doi: https://doi.org/10.1002/bmc.4714

Iwuozor, K. O. *et al.* (2022) 'Removal of pollutants from aqueous media using cow dung-based adsorbents', *Current Research in Green and Sustainable Chemistry,* 5**,** pp**.** 100300. doi: https://doi.org/10.1016/j.crgsc.2022.100300

Jain, M. *et al.* (2022) 'Statistical evaluation of cow-dung derived activated biochar for phenol adsorption: Adsorption isotherms, kinetics, and thermodynamic studies', *Bioresource Technology,* 352**,** pp. 127030. doi: https://doi.org/10.1016/j.biortech.2022.127030

Kandasamy, S. *et al.* (2023) 'Adsorption of methylene blue dye by animal dung biomass–derived activated carbon: optimization, isotherms and kinetic studies', *Biomass Conversion and Biorefinery***,** pp. 1-15. doi: https://doi.org/10.1007/s13399-023-04710-y

Khoon Poh, A. *et al.* (2014) 'Polyurethane wood adhesive from palm oil-based polyester polyol', *Journal of Adhesion Science and Technology,* 28**,** pp. 1020-1033. doi: https://doi.org/10.1080/01694243.2014.883772

Latour, R. A. (2015) 'The Langmuir isotherm: a commonly applied but misleading approach for the analysis of protein adsorption behavior', *Journal of biomedical materials research part A,* 103**,** pp. 949-958. doi: https://doi.org/10.1002/jbm.a.35235

Li, K. *et al.* (2017) 'Preparation of nitrogen-doped cotton stalk microporous activated carbon fiber electrodes with different surface area from hexamethylenetetramine-modified cotton stalk for

electrochemical degradation of methylene blue', *Results in physics,* 7**,** pp. 656-664. doi: https://doi.org/10.1016/j.rinp.2017.01.030

Li, Q. *et al.* (2022) 'Kinetics of the hydrogen absorption and desorption processes of hydrogen storage alloys: A review', *International Journal of Minerals, Metallurgy and Materials,* 29**,** pp. 32-48. doi: https://doi.org/10.1007/s12613-021-2337-8

Liu, Q. *et al.* (2020) 'Edge activation of an inert polymeric carbon nitride matrix with boosted absorption kinetics and near-infrared response for efficient photocatalytic CO_2 reduction', *Journal of Materials Chemistry A,* 8**,** pp. 11761-11772. doi: https://doi.org/10.1039/D0TA03870A

Majd, M. M. *et al.* (2022) 'Adsorption isotherm models: A comprehensive and systematic review (2010− 2020)', *Science of The Total Environment,* 812**,** pp**.** 151334. doi: https://doi.org/10.1016/j.scitotenv.2021.151334

Misran, E. *et al.* (2022) 'Banana stem based activated carbon as a low-cost adsorbent for methylene blue removal: Isotherm, kinetics, and reusability', *Alexandria Engineering Journal,* 61**,** pp**.** 1946-1955. doi: https://doi.org/10.1016/j.aej.2021.07.022

Nowrouzi, M. *et al.* (2017) 'An enhanced counter-current approach towards activated carbon from waste tissue with zero liquid discharge', *Chemical Engineering Journal,* 326**,** pp**.** 934-944. doi: https://doi.org/10.1016/j.cej.2017.05.141

Nowrouzi, M.,Younesi, H., Bahramifar, N. (2018) 'Superior CO_2 capture performance on biomass-derived carbon/metal oxides nanocomposites from Persian ironwood by H_3PO_4 activation', *Fuel,* 223**,** pp. 99-114. doi: https://doi.org/10.1016/j.fuel.2018.03.035

Ofgea, N. M.,Tura, A. M., Fanta, G. M. (2022) 'Activated carbon from H_3PO_4-activated Moringa stenopetale seed husk for removal of methylene blue: optimization using the response surface method (RSM)', *Environmental and Sustainability Indicators,* 16**,** pp**.** 100214. doi: https://doi.org/10.1016/j.indic.2022.100214

Pandey, B. *et al.* (2021) 'Phytostabilization of coal mine overburden waste, exploiting the phytoremedial efficacy of lemongrass under varying level of cow dung manure', *Ecotoxicology and Environmental Safety,* 208, pp. 111757. doi: https://doi.org/10.1016/j.ecoenv.2020.111757

Patty, D. J.,Loupatty, G., Sopalauw, F. (2017) 'Interpretation FTIR spectrum of seawater and sediment in the Ambon Bay (TAD)', *AIP Conference Proceedings,* 1801, pp. 1-6. doi: https://doi.org/10.1063/1.4973109

Peer, F. E.,Bahramifar, N., Younesi, H. (2018) 'Removal of Cd (II), Pb (II) and Cu (II) ions from aqueous solution by polyamidoamine dendrimer grafted magnetic graphene oxide nanosheets', *Journal of the Taiwan Institute of Chemical Engineers,* 87**,** pp. 225-240. doi: https://doi.org/10.1016/j.jtice.2018.03.039

Putranto, A. *et al.* (2022) 'Effects of pyrolysis temperature and impregnation ratio on adsorption kinetics and isotherm of methylene blue on corn cobs activated carbons', *South African Journal of Chemical Engineering,* 42**,** pp. 91-97. doi: https://doi.org/10.1016/j.sajce.2022.07.008

Rajahmundry, G. K. *et al.* (2021) 'Statistical analysis of adsorption isotherm models and its appropriate selection', *Chemosphere,* 276**,** pp. 130176. doi: https://doi.org/10.1016/j.chemosphere.2021.130176

Rajkumar, S. *et al.* (2019) 'Low-cost fluoride adsorbents prepared from a renewable biowaste: syntheses, characterization and modeling studies', *Arabian Journal of Chemistry,* 12**,** pp. 3004-3017. doi: https://doi.org/10.1016/j.arabjc.2015.06.028

Ramutshatsha-Makhwedzha, D. *et al.* (2022) 'Activated carbon derived from waste orange and lemon peels for the adsorption of methyl orange and methylene blue dyes from wastewater', *Heliyon,* 8**,** pp**.** e09930. doi: https://doi.org/10.1016/j.heliyon.2022.e09930

Rani, R. *et al.* (2017) 'Evaluation of anti-diabetic activity of glycyrrhizin-loaded nanoparticles in nicotinamide-streptozotocin-induced diabetic rats', *European Journal of Pharmaceutical Sciences,* 106**,** pp. 220-230. doi: https://doi.org/10.1016/j.ejps.2017.05.068

Rastgar, S. *et al.* (2022) 'Low-cost magnetic char derived from oily sludge for Methylene Blue dye removal: optimization, isotherm, and kinetic approach', *Advances in Environmental Technology,* 8**,** pp. 329-343. doi: https://doi.org/10.22104/AET.2022.5795.1595

Rastgar, S. *et al.* (2023) 'Photocatalytic degradation of methylene blue (MB) dye under UV light irradiation by magnetic diesel tank sludge (MDTS)', *Biomass Conversion and Biorefinery***,** pp. 1-12. doi: https://doi.org/10.1007/s13399-023-04062-7

Rezaei, H.,Rostami, N. M., Abyar, H. (2024) 'Magnetic nanocomposite synthesized from cocopeat for highly efficient mercury removal from aqueous solutions', *Biomass Conversion and Biorefinery***,** pp. 1-13. doi: https://doi.org/10.1007/s13399-024-05425-4

Sahmoune, M. N. (2019) 'Evaluation of thermodynamic parameters for adsorption of heavy metals by green adsorbents', *Environmental Chemistry Letters,* 17**,** pp**.** 697-704. doi: https://doi.org/10.1007/s10311-018-00819-z

Saleh, T. A. (2022). 'Isotherm models of adsorption processes on adsorbents and nanoadsorbents', Interface Science and Technology. 34, pp. 99-126. https://doi.org/10.1016/B978-0-12-849876-7.00009-9

Saraswat, S. K.,Demir, M., Gosu, V. (2020) 'Adsorptive removal of heavy metals from industrial effluents using cow dung as the biosorbent: Kinetic and isotherm modeling', *Environmental Quality Management,* 30**,** pp. 51-60. doi: https://doi.org/10.1002/tqem.21703

Shirmardi, M. *et al.* (2016) 'Removal of atrazine as an organic micro-pollutant from aqueous solutions: a comparative study', *Process Safety and Environmental Protection,* 103**,** pp. 23-35. doi: https://doi.org/10.1016/j.psep.2016.06.014

Shukre, R. *et al.* (2022) 'Thermodynamic modeling of adsorption at the liquid-solid interface', *Fluid Phase Equilibria,* 563**,** pp. 113573. doi: https://doi.org/10.1016/j.fluid.2022.113573

Song, W. *et al.* (2020) 'Enhanced hydrogen absorption kinetics by introducing fine eutectic and long-period stacking ordered structure in ternary eutectic Mg–Ni–Y alloy', *Journal of Alloys and Compounds,* 820**,** pp. 153187. doi: https://doi.org/10.1016/j.jallcom.2019.153187

Subramaniam, R., and Ponnusamy, S. K. (2015) 'Novel adsorbent from agricultural waste (cashew NUT shell) for methylene blue dye removal: Optimization by response surface methodology', *Water Resources and Industry,* 11**,** pp. 64-70. doi: https://doi.org/10.1016/j.wri.2015.07.002

Sun, X. *et al.* (2015) 'Removal of cationic dye methylene blue by zero-valent iron: effects of pH and dissolved oxygen on removal mechanisms', *Journal of Environmental Science and Health, Part A,* 50**,** pp. 1057-1071. doi: https://doi.org/10.1080/10934529.2015.1038181

Tang, X. *et al.* (2021) 'Dynamic pyrolysis behaviors, products, and mechanisms of waste rubber and polyurethane bicycle tires', *Journal of hazardous materials,* 402, pp. 123516. doi: https://doi.org/10.1016/j.jhazmat.2020.123516

Tang, Y. *et al.* (2022) 'Magnetic powdery acrylic polymer with ultrahigh adsorption capacity for atenolol removal: Preparation, characterization, and microscopic adsorption mechanism', *Chemical Engineering Journal,* 446**,** pp. 137175. doi: https://doi.org/10.1016/j.cej.2022.137175

Tran, H. N. (2022) 'Is it possible to draw conclusions (adsorption is chemisorption) based on fitting between kinetic models (pseudo-second-order or elovich) and experimental data of time-dependent adsorption in solid-liquid phases?', *Recent Innovations in Chemical Engineering* 15, pp. 228-230. doi: https://doi.org/10.2174/2405520416666221202085740

Tsai, W.-T.,Hsu, C.-H., Lin, Y.-Q. (2019) 'Highly porous and nutrients-rich biochar derived from dairy cattle manure and its potential for removal of cationic compound from water', *Agriculture,* 9**,** pp**.** 114. doi: https://doi.org/10.3390/agriculture9060114

Udayakumar, M. *et al.* (2021) 'Synthesis of activated carbon foams with high specific surface area using polyurethane elastomer templates for effective removal of methylene blue', *Arabian Journal of Chemistry,* 14**,** pp. 103214. doi: https://doi.org/10.1016/j.arabjc.2021.103214

Valderrama, C. *et al.* (2010) 'Kinetic evaluation of phenol/aniline mixtures adsorption from aqueous solutions onto activated carbon and hypercrosslinked polymeric resin (MN200)', *Reactive and Functional Polymers,* 70**,** pp. 142-150. doi: https://doi.org/10.1016/j.reactfunctpolym.2009.11.003

Van Phuong, N., and Hoang, N. K. (2021) 'Assessment of cadmium ion adsorption capacity in water by biochar produced from pyrolysis of

cow dung', *International Journal,* 9**,** pp. 203-210. doi: https://doi.org/10.30534/ijeter/2021/09932021

Vyawahare, P. *et al.* (2022) 'From langmuir isotherm to brunauer–emmett–teller isotherm', *AIChE Journal,* 68**,** pp**.** e17523. doi: https://doi.org/10.1002/aic.17523

Xiu, L. *et al.* (2020) 'Exopolysaccharides from Lactobacillus kiferi as adjuvant enhanced the immuno-protective against Staphylococcus aureus infection', *International Journal of Biological Macromolecules,* 161**,** pp. 10-23. doi: https://doi.org/10.1016/j.ijbiomac.2020.06.005

Yusop, M. F. M. *et al.* (2021) 'Adsorption of cationic methylene blue dye using microwave-assisted activated carbon derived from acacia wood: optimization and batch studies', *Arabian Journal of Chemistry,* 14**,** pp. 103122. doi: https://doi.org/10.1016/j.arabjc.2021.103122

Yusop, M. F. M.,Aziz, A., Ahmad, M. A. (2022) 'Conversion of teak wood waste into microwave-irradiated activated carbon for cationic methylene blue dye removal: optimization and batch studies', *Arabian Journal of Chemistry,* 15**,** pp. 104081. doi: https://doi.org/10.1016/j.arabjc.2022.104081

Zhu, Y. *et al.* (2018) 'Removal of methylene blue from aqueous solution by cattle manure-derived low temperature biochar', *RSC advances,* 8**,** pp. 19917-19929. doi: https://doi.org/10.1039/C8RA03018A